EurJIC
European Journal of Inorganic Chemistry

Research Article
doi.org/10.1002/ejic.202300144

Chemistry Europe
European Chemical Societies Publishing

www.eurjic.org

Syntheses, Characterization, and DNA Binding Studies of a Series of Copper(II), Nickel(II), Platinum(II) and Zinc(II) Complexes Derived from Schiff Base Ligands

Valentina Iannace,[a, b] Ferran Sabaté,[a] Molly Bartlett,[c] Jessica Berrones Reyes,[c] Ariadna Lázaro,[a, d] Alessia Fantoni,[b] Ramon Vilar,*[c] Laura Rodríguez,*[a, d] and Antonella Dalla Cort*[b]

Three series of metal salophen complexes derived from Zn^{2+}, Cu^{2+}, Pt^{2+} and Ni^{2+} have been synthesized and their interaction with quadruplex DNA has been evaluated. The compounds differ on the number of ethyl piperidine substituents. They have been characterized by ^{1}H NMR, IR and UV-visible spectroscopies and by HR-mass spectrometry. Their luminescent properties have been also evaluated and we can observe that, as expected, Zn^{2+} and Pt^{2+} complexes are those displaying more interesting luminescence with an emission band red-shifted with respect to the corresponding uncoordinated ligand. DNA interactions with G4 and duplex DNA were evaluated by FRET melting assays (for the Zn^{2+}, Cu^{2+} and Ni^{2+} complexes) and by emission titrations (for one Pt^{2+} complex) which indicated that the disubstituted compounds **2-Ni** and **2-Pt** are the only ones that display good affinity for G4 DNA structures.

Introduction

Schiff bases have played a major role as polydentate ligands in coordination chemistry due to the fact that they easily form stable complexes with many transition and main group metal ions.[1] Such derivatives have shown a wide variety of applications in catalytic,[2] synthetic,[3] industrial,[4] biochemical[5] and biological processes.[6] One particular class of Schiff bases are the tetradentate salen and salophen ligands (Figurea 1a) which can be synthesized via condensation reactions between salicyladehyde and the corresponding diamines. The resulting metal complexes with these tetradentate ligands, have been extensively studied as DNA binders and potential drugs. Initial investigations by Burrows[7,8] showed metal-salen complexes (with M = Ni^{2+}, Cu^{2+} and Mn^{3+}) to bind non-covalently to duplex DNA and induce strand scission. Subsequently square planar (with M = Ni^{2+}, Cu^{2+} and Pt^{2+}) and square-based pyramidal (with M = VO^{+}) metal-salophen complexes were shown to be excellent binders towards telomeric (HTelo) G-quadruplex DNA ;[9–11] other studies showed the ability of this general class of metal complexes to bind (in some cases selectively) to other G-quadruplex DNA structures .[12–15] G-quadruplexes (G4s) are non-canonical tetra-stranded DNA structures that form in guanine rich regions of the genome. There is growing evidence that such structures have important biological roles in telomere maintenance, transcription and replication.[16–18] Therefore, small molecules able to selectively bind to these tetra-stranded structures could have potential therapeutic applications .[19,20]

Based on our long-standing interest in these compounds and in their supramolecular chemistry[21,22] including their use in molecular recognition[23] and catalytic processes,[2] and their demonstrated ability to bind to G4 DNA (see above) we decided to prepare a series of new derivatives to explore two features: i) the effect that a negatively charged group (i.e. COO^{-}) in the backbone of the salophen ligand would have on the selectivity of the resulting metal complexes towards G4 DNA over duplex DNA. Since DNA is an overall negatively charged molecule, a negative group should in principle reduce the non-specific binding of the complex towards DNA. We hypothesised that this could potentially reduce its ability to intercalate into duplex DNA but still allow it to end-stack onto G4 DNA improving its

[a] V. Iannace, Dr. F. Sabaté, Dr. A. Lázaro, Prof. L. Rodríguez
Departament de Química Inorgànica i Orgànica, Secció de Química Inorgànica
Universitat de Barcelona
Martí i Franquès 1–11, E-08028 Barcelona (Spain)
E-mail: laura.rodriguez@qi.ub.es

[b] V. Iannace, A. Fantoni, Prof. A. Dalla Cort
Dipartimento di Chimica
Università degli Studi di Roma "La Sapienza"
Rome (Italy)
E-mail: antonella.dallacort@uniroma1.it

[c] M. Bartlett, Dr. J. Berrones Reyes, Prof. R. Vilar
Department of Chemistry
Imperial College London
Molecular Sciences Research Hub White City Campus
82 Wood Lane, London W12 0BZ (United Kingdom)
E-mail: r.vilar@imperial.ac.uk

[d] Dr. A. Lázaro, Prof. L. Rodríguez
Institut de Nanociència i Nanotecnologia (IN2UB)
Universitat de Barcelona
08028 Barcelona (Spain)

Supporting information for this article is available on the WWW under https://doi.org/10.1002/ejic.202300144

Research Article
doi.org/10.1002/ejic.202300144

selectivity; ii) the number of ethyl piperidine groups attached to the salophen. Cyclic amines such as piperidine are protonated at physiological pH increasing the water solubility of the corresponding polyaromatic metal complexes and increasing their affinity towards DNA due to their interactions with the phosphate backbone. Most of the previously reported metal complexes with salophens containing piperidine groups, are doubly substituted; no study has looked at the effect that removing one of the two would have on DNA affinity, and more importantly, selectivity. With this in mind, herein, we report the synthesis, characterization, and DNA binding properties of a number of metal-salophen complexes with M = Zn^{2+}, Cu^{2+}, Pt^{2+} and Ni^{2+} (see Figure 1b).

Results and Discussion

The syntheses of the metal complexes were carried out through the preliminary formation of the corresponding salophen ligand and subsequent reaction with the corresponding metal salt (method A for **1M** and **3M** complexes) or by one pot reaction mixing the corresponding aldehyde, diamine and metal salt (method B). Complexes **2M** can be also obtained through the reaction of the previously synthesized **1M** complexes and 1-(2-chloroethyl)piperidine hydrochloride (see Schemes 1–3). Better results were obtained for one pot reactions (Method B) in the case of **2M** and **3M**. Unfortunately, the synthesis of the asymmetric Pt complex **3Pt** was not reproducible and for this reason it was not considered in this work.

Characterization by ^{1}H NMR and IR spectroscopy, mass spectrometry and elemental analyses confirmed the formation of the compounds in all cases (see Experimental Section and Supporting Information). In particular, the ^{1}H NMR spectra of the compounds show the appearance of the imine proton (and disappearance of the aldehyde proton) as a clear indication of the formation of the salophen ligand. This was also confirmed by the disappearance of the C=O stretching frequency from the aldehyde in the corresponding IR spectra. The successful formation of the metal complexes was evidenced by different spectroscopic techniques (^{1}H NMR, IR), mass spectrometry and elemental analyses. In particular, the corresponding ^{1}H NMR spectra display slight downfield shifts for the imine and aromatic protons closer to the metal coordination point and the presence of the piperidine protons for Series 2 and 3.

Photophysical characterization

Absorption and emission spectra of all compounds (**series 1**–**3** and organic precursors **L1**–**L3**) were recorded in DMSO and the results are summarized in Table 1 and Figures 2, 3 and S30-31. The absorption spectra of the compounds display different bands between *ca.* 320 and 490 nm which can be assigned to $\pi\rightarrow\pi^*$ transitions of the phenyl ring and of the azomethine chromophore. Additional high energy $\pi\rightarrow\pi^*$ transitions around 260 nm have been recorded for the metal complexes. The farthest energy band is assigned to $n\rightarrow\pi^*$ transition involving the promotion of the lone pair electrons of nitrogen atom to the anti-bonding π^* orbital, according to literature.[22,24–27]

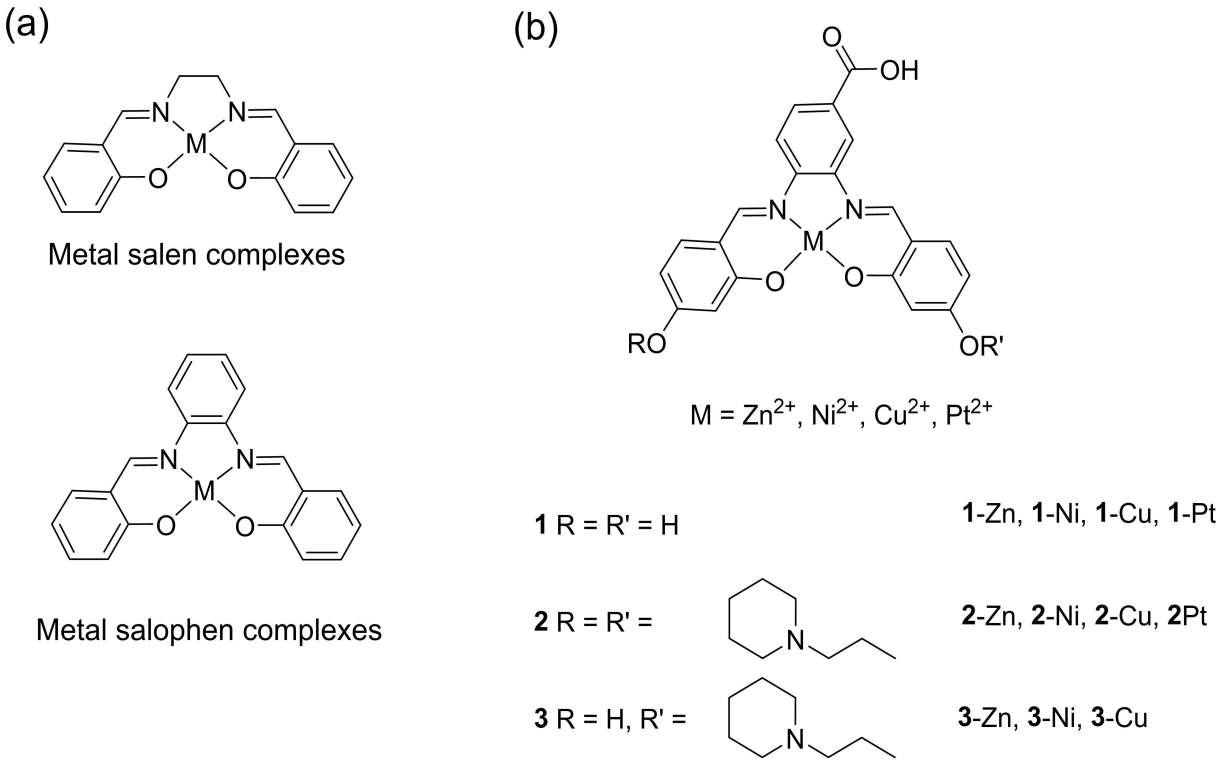

Figure 1. (a) General chemical structure of metal salen and metal salophen complexes; (b) the specific metal salophen complexes reported in this work.

Research Article
doi.org/10.1002/ejic.202300144

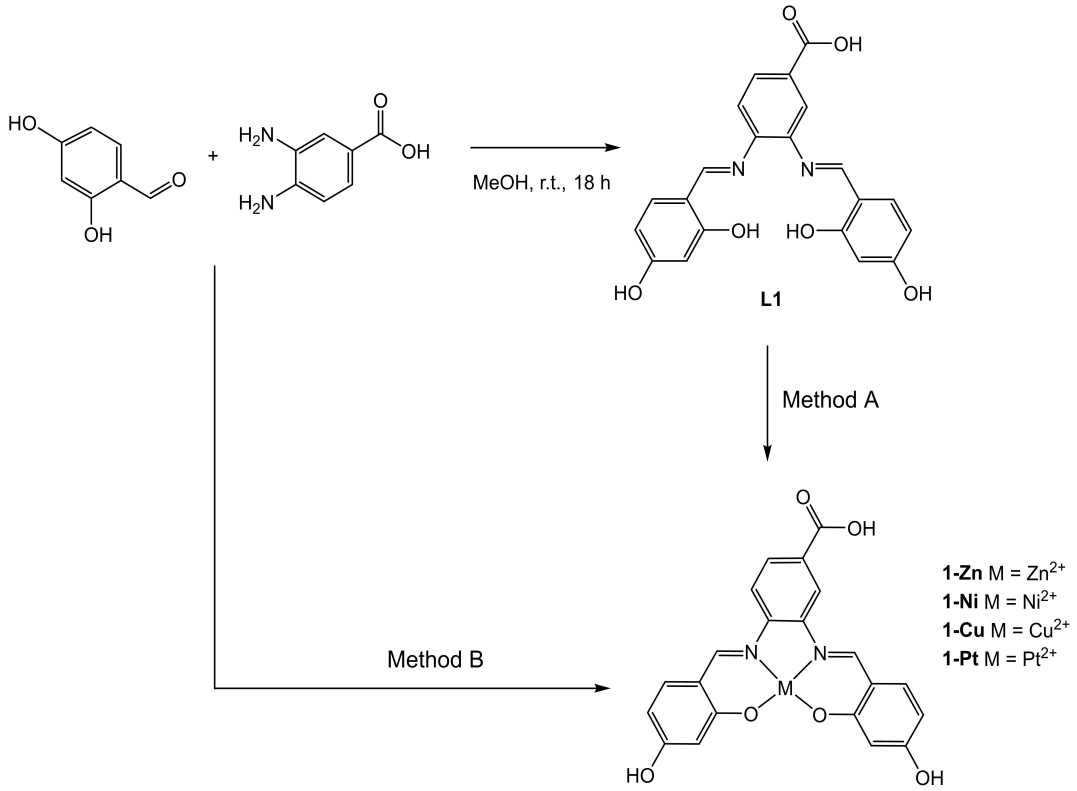

Scheme 1. Synthesis of **1M** (M = Zn^{2+}, Ni^{2+}, Cu^{2+} and Pt^{2+}) complexes. Method A consists in a two-step reaction, i.e. preparation and isolation of the ligand, and its reaction with the desired salt. Method B, instead, uses a one-pot procedure, as described further on.

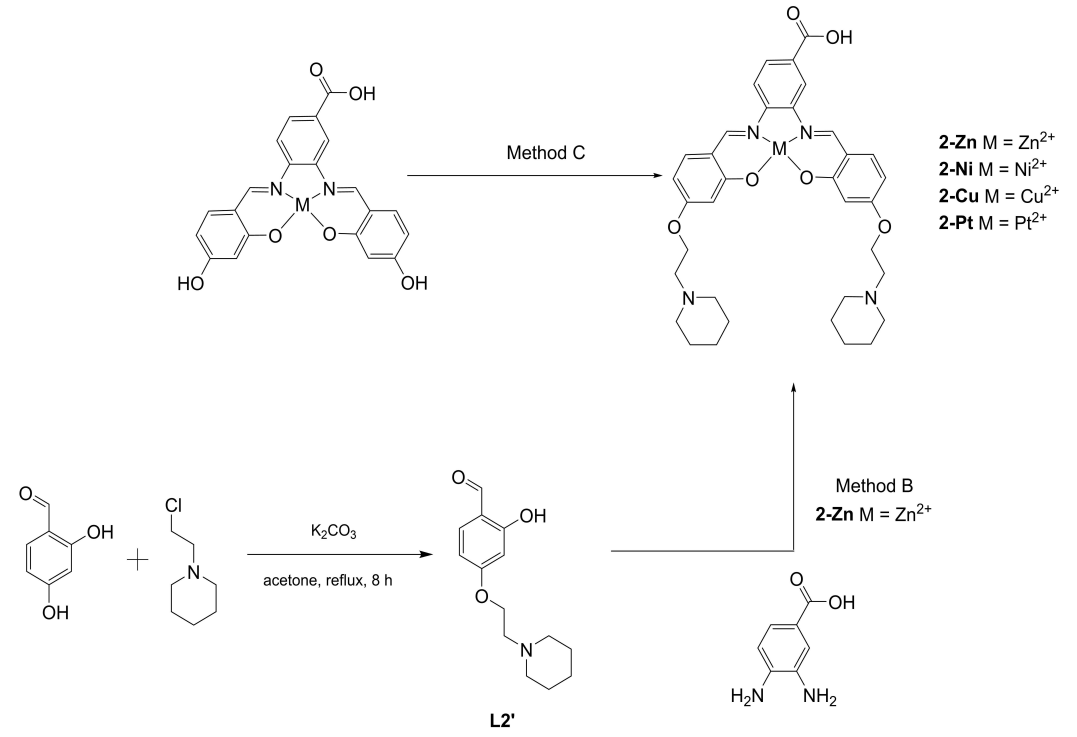

Scheme 2. Synthesis of **2M** (M = Zn^{2+}, Ni^{2+}, Cu^{2+} and Pt^{2+}) complexes. Method C consists in the direct functionalization of the preformed metal complex.

Research Article
doi.org/10.1002/ejic.202300144

Chemistry Europe
European Chemical Societies Publishing

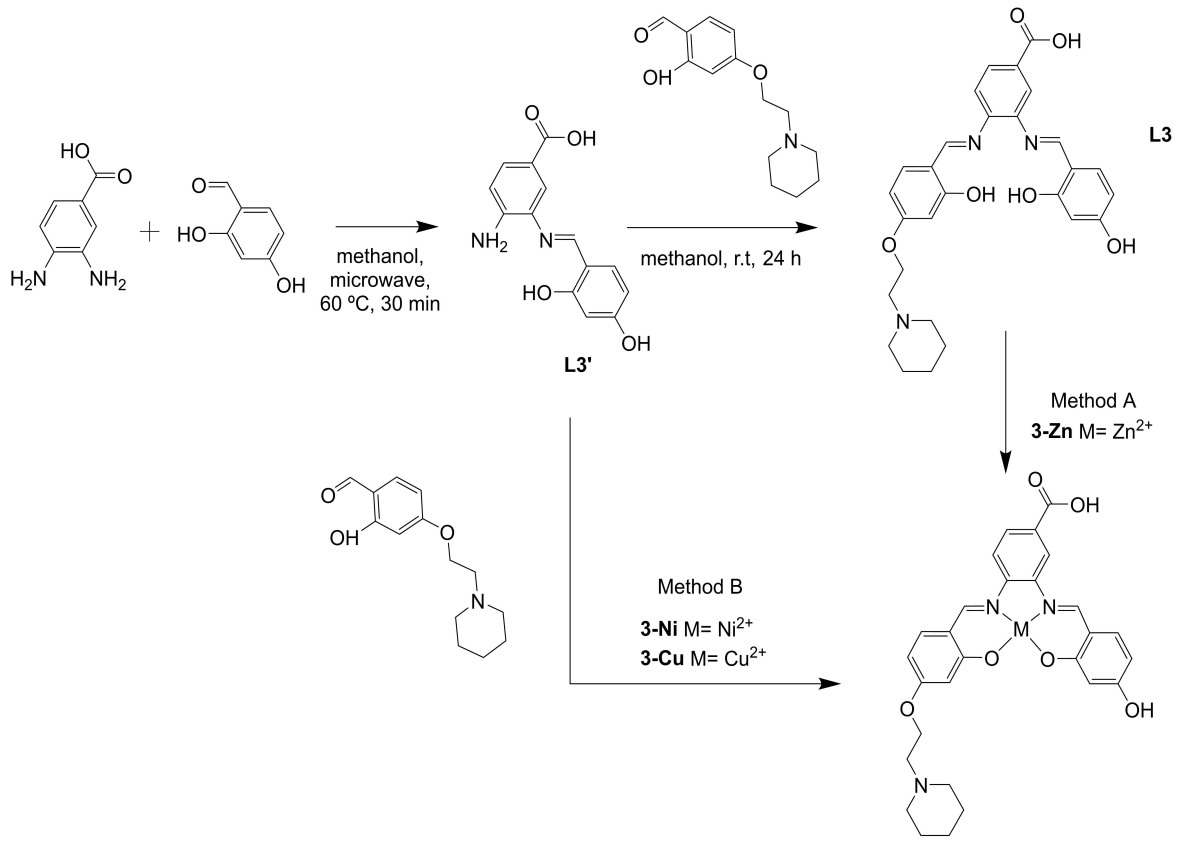

Scheme 3. Synthesis of **3-M** (M = Zn^{2+}, Ni^{2+} and Cu^{2+}) complexes.

Table 1. Spectral data including wavelength absorption, molar extinction coefficients, ε (in brackets), emission maxima and luminescence quantum yields obtained in dimethylsulfoxide solutions.

Compound	λ_{abs} [nm] ($\varepsilon \times 10^{-3}$, $M^{-1}cm^{-1}$)	λ_{em}^{max} [nm]	Φ
L1	337 (40.9)	493[a]	0.06
L3	333 (34.8)	468[a]	0.09
1-Zn	266 (17.1), 320 (24.6), 398 (28.5), 437 (19.9)	502[b]	0.01
1-Ni	265 (25.0), 318 (22.4), 392 (27.1), 459 (14.4)	–	–
1-Cu	269 (21.2), 328 (22.5), 406 (26.5)	–	–
1-Pt	318 (19.0), 377 (26.8), 440 (17.8), 489 (9.8)	580[b]	0.02
2-Zn	267 (20.7), 317 (28.7), 399 (33.7), 440 (21.7)	508[b]	0.02
2-Ni	264 (36.5), 319 (30.3), 389 (33.8), 464 (18.1)	–	–
2-Cu	270 (37.1), 328 (43.9), 407 (33.1)	–	–
2-Pt	321 (25.6), 382 (29.2), 445 (20.9), 503 (10.6)	592[b]	0.01
3-Zn	268 (16.2), 317 (22.8), 398 (25.4), 440 (16.4)	509[b]	0.01
3-Ni	266 (16.2), 318 (25.3), 389 (28.8) 458 (15.7)	–	–
3-Cu	270 (29.2), 337 (40.9), 393 (21.8), 466 (12.9)	–	–

[a] λ_{exc} = 335 nm, [b] λ_{exc} = 380 nm.

Excitation of the samples at the lowest energy transition give rise to a broad emission band attributed to single state transitions.[22,24–32] This band is red-shifted in the case of the metal complexes (Figures 3 and S31) with particularly longer wavelength emission in the case of platinum(II) complexes with typical emissions around 580 nm.[33] No significant emission was recorded for nickel(II) and copper(II) complexes, as expected for this type of metal derivatives. Luminescence quantum yields are moderate-low, around 1% for the Zn^{II} and Pt^{II} complexes and 6–9% for the uncomplexed ligands, as expected for heavy atom derivatives.

DNA binding studies: FRET melting assays

To evaluate the ability of the different Ni^{2+}, Cu^{2+} and Zn^{2+} complexes to interact with G-quadruplex DNA (in particular, with *c-myc* G4 DNA), FRET melting experiments were performed

Research Article
doi.org/10.1002/ejic.202300144

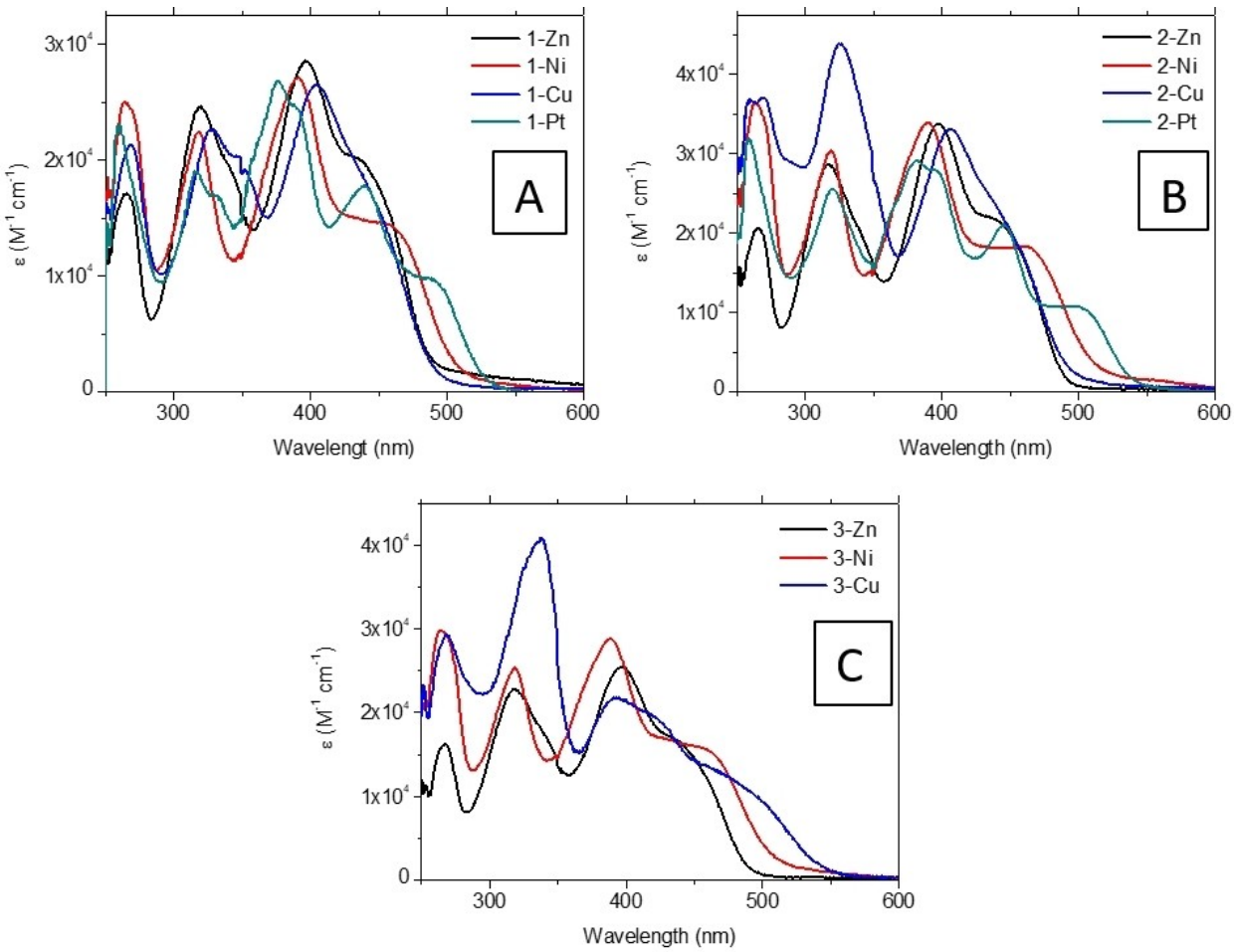

Figure 2. Absorption spectra for 1×10^{-5} M dimethyl sulfoxide solutions of compounds from series **1** (A), series **2** (B) and series **3** (C).

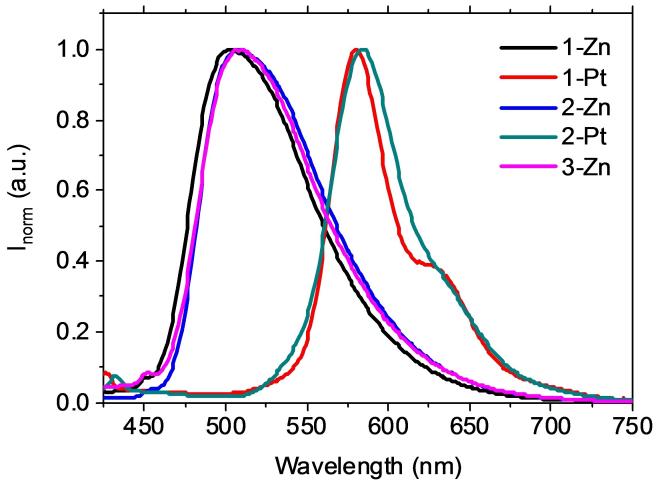

Figure 3. Normalized emission spectra for 1×10^{-5} M dimethyl sulfoxide solutions of compounds **1–3**.

(note that the Pt^{2+} complexes were not investigated by FRET since their emission interferes with the assay – instead, the interaction of one of these complexes, **2-Pt**, with DNA was investigated by emission titrations as discussed below). The results indicate that only the complex **2-Ni** induced significant thermal stabilization of the G4 structure when [Ligand]/[Oligo] ratio is 10:1 ($\Delta T_m = 8.0 \pm 1.9$ °C) and 20:1 ($\Delta T_m = 17.4 \pm 1.9$ °C). These FRET results suggest that the structure and geometry given by the nickel(II) center confers the optimal characteristics for π–π stacking to the guanine quartet. The different substitution patterns lead to significant variations in binding within the Ni(II) series (Figure 4).

To study further the selectivity displayed by **2-Ni** for G4 s in the presence of excess duplex DNA (ct-DNA and st-DNA), FRET melting competition assays were carried out. In this experiment the FRET melting temperature of the doubly labelled G4 (FAM-*cMyc*-TAMRA) was obtained in the presence of a fixed concentration of the compound (2 μM) and in the presence of increasing amounts of non-labelled double strand DNA (0-120 μM). The findings for **2-Ni** (Figure 5) demonstrate that this complex has high selectivity for G4 DNA structure over duplex DNA since even in the presence of a large excess (60-fold) of duplex DNA (ct-DNA and st-DNA), the melting temperature of the G4 continued practically unaffected.

Research Article
doi.org/10.1002/ejic.202300144

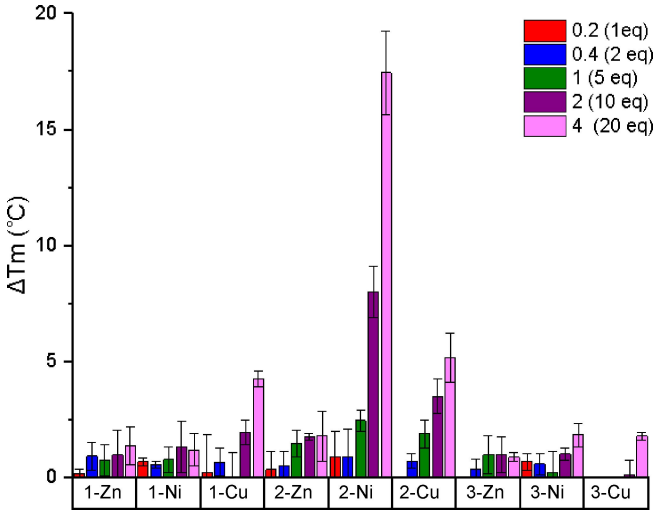

Figure 4. ΔTm (°C) values for *c-Myc* G4 DNA (0.4 μM) plotted in presence of increasing amounts of the corresponding complexes. Results were obtained by averaging three independent experiments.

DNA binding affinity of complex 2-Pt

Having established that **2-Ni** is the best G4 DNA binder, it was of interest to study a broader range of G4 topologies and determine the binding affinities (rather than the thermal stabilization). As mentioned above, the **2-Pt** analogue is an emissive compound which cannot be studied by FRET since it interferes with the FAM-TAMRA pair. On the other hand, upon interaction with DNA, **2-Pt** switches-on its emission intensity therefore, its binding affinity can be determined by emission spectroscopy (i.e. by titrating the complex with an increasing amount of DNA and measuring changes in its emission). This complex was screened against eight different DNA targets including a range of G4 topologies and duplex DNA (see Figure 6). The results show that **2-Pt** is a good G4 DNA binder and has some selectivity (one order of magnitude) for quadruplex over duplex DNA. The affinity of **2-Pt** to *c-myc* G4 DNA (5.38×10^6 M^{-1}) was consistent with the thermal stabilization induced by the nickel(II) analogue (**2-Ni**) determined by FRET melting (see above).

Docking studies between DNA and 2-Pt

In order to gain a better understanding of the DNA binding modes of the square planar **2-Pt** complex, molecular docking studies were performed. These studies confirmed that for *HTelo*, *c-myc* and *kras* G4 DNA structures, **2-Pt** binds to the end G-quartet through effective π-π stacking interactions (see Figure 7 a,b for *c-myc* and ESI for all other G4 s). Interestingly, docking for G4 sequences with lower binding affinities towards **2-Pt** (see Figure S36) suggests that access to the G-quartet is hindered, resulting in slightly weaker binding interactions between these G4 s and **2-Pt**. In all cases hydrogen bonding interactions were detected between the DNA and the protonated piperidine. For *c-myc*, *kras*, *BCL2*, and *ckit2* G4 DNA docking showed that the deprotonated carboxylic acid also participates in hydrogen bonding.

Our initial hypothesis was that the charged carboxylic acid would reduce duplex DNA intercalation by repelling the negatively charged phosphate backbone – and indeed, our FRET melting data with **2-Ni** and emission titration data for **2-Pt** indicates lower affinity for duplex than for G4 DNA. However, the docking studies indicated that the complex can intercalate into duplex DNA and the carboxylate is involved in close-contact interactions (green area on molecular surface, Figure 6c,d).

Conclusions

The syntheses of Zn^{2+}, Cu^{2+}, Pt^{2+} and Ni^{2+} salophen complexes with or without a carboxylic substituent on the phenyl backbone of the salophen, and one or two ethyl-piperidine substituents have been performed. This has been successfully achieved by either synthesising the ligand first and then coordinating the metal centre, or by one-pot synthetic approach. This second methodology has been observed to induce better yields for piperidine derivatives. Zn^{2+} and Pt^{2+}

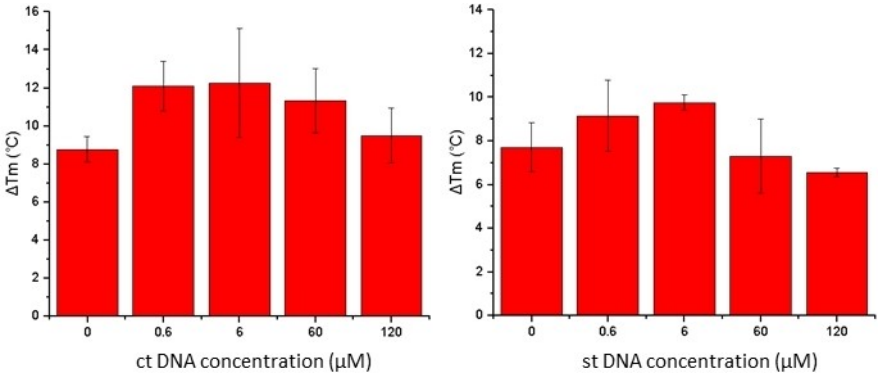

Figure 5. FRET competition experiments using FAM-*cMyc*-TAMRA G4 DNA (0.2 μM) and **2-Ni** (2 μM) with increasing concentrations (0–120 μM) of duplex DNA (ct-DNA and st-DNA).

Research Article
doi.org/10.1002/ejic.202300144

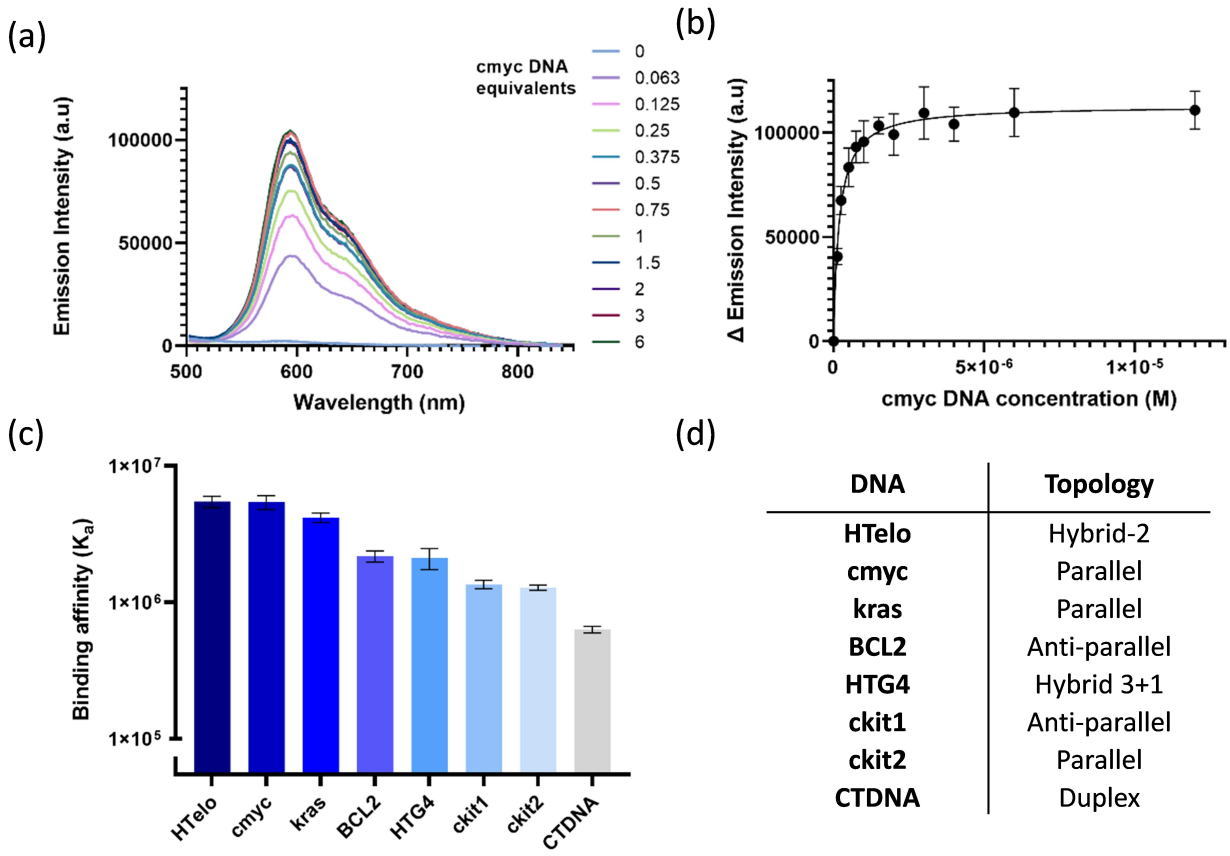

DNA	Topology
HTelo	Hybrid-2
cmyc	Parallel
kras	Parallel
BCL2	Anti-parallel
HTG4	Hybrid 3+1
ckit1	Anti-parallel
ckit2	Parallel
CTDNA	Duplex

Figure 6. DNA binding affinity of complex 2-Pt. (a) Emission spectra showing the increase of intensity upon addition of increasing amounts of c-myc DNA to a solution containing 2-Pt (2 μM); (b) binding curve generated from the emission spectra recorded at 592 nm (R2: 0.94); (c) bar chart plot showing the binding affinity constants for 2-Pt with a range of DNA target; (d) table stating the topology of each DNA sequence investigated.

complexes display luminescent properties with similar emission quantum yields but with longer emission wavelengths for Pt^{2+} derivatives.

Their DNA binding properties were evaluated by FRET melting assays for the Zn^{2+}, Cu^{2+} and Ni^{2+} derivatives, and via emission titrations with one of the Pt^{2+} complexes (**2-Pt**). These data indicate that the compounds have generally poor or only modest G4 DNA binding properties. The best G4 DNA binders are the disubstituted Ni^{2+} and Pt^{2+} complexes **2-Ni** and **2-Pt**, followed by the **2-Cu** complex (all other compounds, do not display significant thermal stabilisation of G4 DNA). This is consistent with previous work that has shown the square planar nickel(II) and platinum(II) cores to be particularly suitable for optimal π-π stacking with the G-tetrad.[9,10] Furthermore, as has been previously documented, the ethyl-piperidine substituents are important to display extra non-covalent interactions (especially when protonated at physiological pH) with DNA. Our initial hypothesis was that the presence of the negatively charged COO^- group in the central ring of the salophen, would increase the selectivity for G4 over duplex DNA by preventing the complex from intercalating into duplex DNA (while still 'allowing' the complex to stack on top of external G4 tetrads). This hypothesis was demonstrated for **2-Ni** (the only complex in this series with significant affinity for G4 DNA) which displays the same ΔT_m for *c-myc* G4 DNA even after addition of an excess of duplex DNA. On the other hand, the emission titrations with **2-Pt** showed that while this complex has higher affinity for G4 DNA, it also binds (with one order of magnitude lower affinity) to duplex DNA. The effect of the COO^- negative charge becomes dominant for **3-Ni** and **3-Cu** (with only one ethyl-piperidine substituents) since these compounds are not able to stabilise G4 DNA – i.e. the negative charge likely prevents the interaction.

Experimental Section

General Procedures

All reagents and solvents were obtained from commercial sources and used as received. All manipulations under N_2 were performed using standard Schlenk techniques with solvents distilled from appropriated drying agents.

NMR spectra were carried out in $CDCl_3$ at the Unitat de RMN of Universitat de Barcelona using a Mercury 400 spectrometer (^1H, 400 MHz; ^{13}C, 100 MHz). Chemical shifts are given in δ values (ppm) relative to TMS and coupling constants J are given in Hz. Electrospray mass spectra were performed at the Unitat d'Espectrometria de Masses at Universitat de Barcelona by introducing the sample in H_2O–CH_3CN 1:1 in an LC/MSD-TOF. Infrared spectra were recorded

Research Article
doi.org/10.1002/ejic.202300144

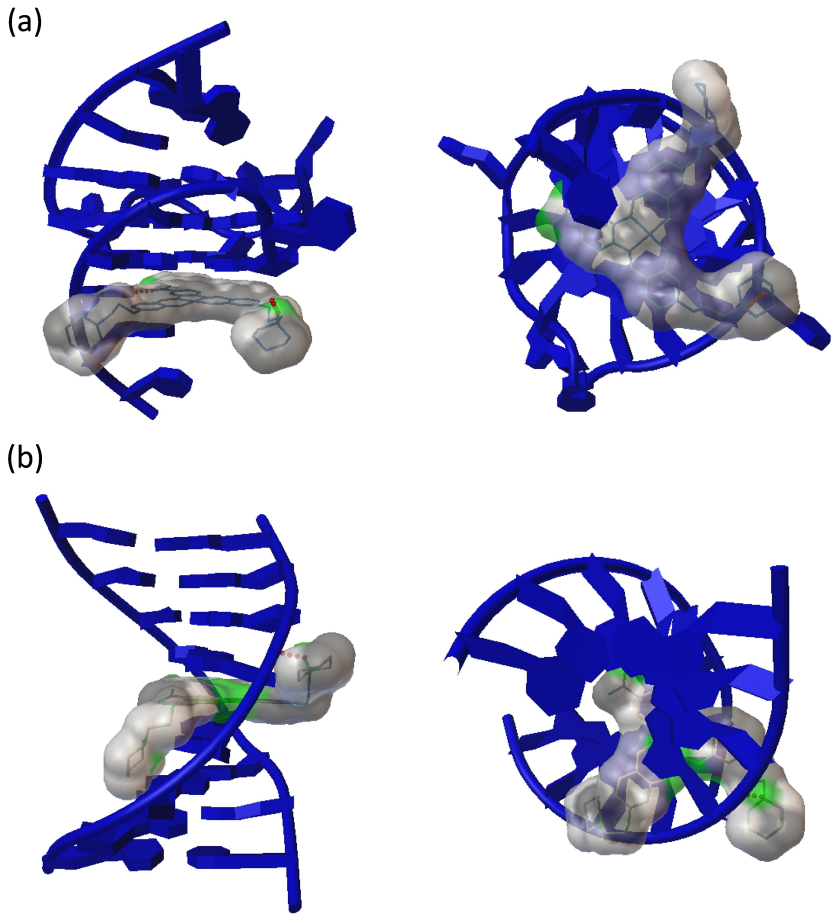

Figure 7. Docking studies (with AutoDock4) between **2-Pt** and DNA to determine the complex's binding mode. (a) Two views of the interaction with *c-myc* DNA (PDB: 2 L7 V); (b) two views of the interaction with duplex DNA (PDB: 1XRW).

on a FT-IR 520 Nicolet spectrophotometer and frequencies are given in cm^{-1}.

UV/Visible absorption spectra were recorded in dimethyl sulfoxide on a Cary 100 scan 388 Varian UV spectrometer. Emission and excitation spectra were recorded in a Horiba Jobin-Yvon SPEX Nanolog-TM spectrofluorimeter at 298 K using 1×10^{-5} M solutions. Emission quantum yields were determined with a Hamamatsu Quantaurus QY absolute photoluminescence quantum yield spectrometer C11347.

Preparation of 1-M Complexes

Method A

Synthesis of (3,4-bis ((E)-2,4-dihydroxybenzylidenamino) benzoic acid (L1)

In a 50 mL flask, 440 mg (3,2 mmol) of 2,4-dihydroxybenzaldehyde were dissolved in 10 mL of methanol. Afterwards, 244 mg (1,60 mmol) of 3,4-diamino benzoic acid were added to the solution. The mixture was stirred at room temperature for 18 hours and a precipitate was formed. The yellow solid was filtered and dried under vacuum. Yield: 350 mg (56%). **^{1}H NMR** (400 MHz, DMSO-d_6): δ 13.19 (s, 1H, Ar–OH), 13.09 (s, 1H, Ar–OH), 12.99 (s br, 1H, COOH), 10.34 (s, Ar–OH), 10.27 (s, Ar–OH), 8.83 (s, 1H, HC=N), 8.82 (s, 1H, HC=N), 7.40-7.50 (m, 3H, ArH), 6.37 (m, 2H, ArH), 6.27 (m, 2H, ArH). **MS-ESI$^+$**: *m/z* 393.11 $[M+H]^+$ (calc: 393.10). **IR**: υ 3700–2400 (O–H), 1593.95 (C=O), 1567.41 (C=N). **Anal. Found**. (calcd for $C_{21}H_{16}N_2O_6$): C 64.36 (64.28), H 4.08 (4.11), N 7.12 (7.14).

Synthesis of 1-Zn

In a 30 mL flask, 100 mg (0.25 mmol) of **L1** were dissolved in 5 mL of methanol and a solution of 55 mg (0,25 mmol) of $Zn(O_2CCH_3)_2 \cdot 2H_2O$ in 5 mL of methanol was added. The mixture was stirred under reflux for 1 hour and a precipitate was formed. The yellow solid was filtered, washed with cold methanol and dried under vacuum. Yield: 82 mg (69%). **^{1}H NMR** (400 MHz, DMSO-d_6): δ 12.94 (s br, 1H, COOH), 9.87 (s, 1H, Ar–OH), 9.77 (s, 1H, Ar–OH), 8.85 (s, 2H HC=N), 8.24 (d, 1H Ar–H), 7.79 (m, 2H, Ar–H), 7.30 (d, 1H, Ar–H), 7.21 (d, 1H Ar–H) 6.02-6.07 (m, 4H, Ar–H). **^{13}C NMR** (100 MHz, DMSO-d_6): δ 175.09, 167.15, 164.40, 163.96, 161.89, 161.23, 143.24, 139,27, 138.41, 138.35, 127.77, 126.84, 116.58, 115.76, 114.01, 113.91, 106.39, 105.37, 104.92. **MS-ESI$^+$**: *m/z* 455.03 $[M+H]^+$ (calc: 455.02). **IR**: υ 3700–2400 (O–H), 1611.64 (C=O), 1582.15 (C=N). **Anal. Found**. (calcd for $C_{21}H_{14}N_2O_6Zn{\cdot}0.5H_2O$): C 54.15 (54.27), H 3.24 (3.25), N 6.07 (6.03).

Synthesis of 1-Ni

Compound **1-Ni** was obtained as a red solid using the same procedure from 100 mg (0.25 mmol) of **L1** and 64 mg (0.25 mmol) of $Ni(O_2CCH_3)_2 \cdot 4H_2O$ as a metal salt. Yield: 109 mg (75%). **^{1}H NMR**

Research Article
doi.org/10.1002/ejic.202300144

(400 MHz, DMSO-d_6): δ 10.48 (s, 1H, Ar–OH), 10.37 (s, 1H, Ar–OH), 8.67 (s, 1H HC=N), 8.61 (s, 1H HC=N), 8.52 (s, 1H, Ar–H), 8.08 (d, 1H, Ar–H), 7.77 (d, 1H Ar–H), 7.54 (d, 1H, Ar–H), 7.44 (d, 1H Ar–H), 6.21-6.27 (m, 4H Ar–H). **MS-ESI$^+$**: *m/z* 449.03 $[M+H]^+$ (calc: 449.03). **IR**: υ 3700–2400 (O–H), 1605.74 (C=O), 1572.66 (C=N). **Anal. Found**. (calcd for $C_{21}H_{14}N_2O_6Ni{\cdot}H_2O$): C 53.84 (54.00), H 3.47 (3.45), N 6.01 (6.00).

Synthesis of 1-Cu

Compound **1-Cu** was obtained as a dark brown solid using the same procedure from 100 mg (0.25 mmol) of **L1** and 50 mg (0.25 mmol) of $Cu(O_2CCH_3)_2{\cdot}H_2O$ as a metal salt. Yield: 93 mg (79%). **MS-ESI$^+$**: *m/z* 454.03 $[M+H]^+$ (calc: 454.02). **IR**: υ 3700–2400 (O–H), 1611.64 (C=O), 1573.31 (C=N). **Anal. Found**. (calcd for $C_{21}H_{14}N_2O_6Cu{\cdot}2.5H_2O$): C 50.34 (50.55), H 3.83 (3.84), N 5.59 (5.61).

Synthesis of 1-Pt

To a solution of **L1** (47 mg, 0.12 mmol) in dimethyl sulfoxide, a solution of K_2CO_3 (33 mg, 0.24 mmol) in water was added dropwise. Afterwards, K_2PtCl_4 (50 mg, 0.12 mmol) dissolved in water was added dropwise to the mixture. The solution was heated 5 h at 60 °C and a precipitate was obtained. The red solid was filtered, washed with water and cold methanol and dried under vacuum. Yield: 58 mg (82%). **^{1}H NMR** (400 MHz, DMSO-d_6): δ 10.46 (s br, Ar–OH, 2H). 9.20 (d, C=NH, 2H), 8.68 (s, Ar–H, 1H), 8.20 (d, Ar–H, 1H), 7.81 (d, Ar–H, 2H), 7.65 (d, Ar–H, 1H), 6.43 (s, Ar–H, 2H), 6.35-6.30 (m, Ar–H, 2H). **MS-ESI$^+$**: *m/z* 586.06 $[M+H]^+$ (calc: 586.06). **IR**: υ 3700–2400 (O–H), 1612.11 (C=O), 1590.32 (C=N). **Anal. Found**. (calcd for $C_{21}H_{14}N_2O_6Pt{\cdot}H_2O$): C 42.10 (41.80), H 2.65 (2.67), N 4.66 (4.64).

Preparation of Complexes 2-M

Method B

To a solution with 2 equivalents of 2,4-dihydroxybenzaldehyde in methanol, 1 equivalent of 3,4-diaminobenzoic acid and 1 equivalent of the target metal salt ($Zn(O_2CCH_3)_2 \cdot 2\ H_2O$, $Ni(O_2CCH_3)_2{\cdot}4\ H_2O$ and $Cu(O_2CCH_3)_2{\cdot}H_2O$) were added respectively. The resulting solution was then stirred at room temperature for 24 h and the complex was isolated by filtration. Yield: 98% (**1-Zn**), 58% (**1-Ni**), 45% (**1-Cu**).

For the platinum derivative, K_2PtCl_4 and sodium acetate (1:4.5 molar ratio) were dissolved in a dimethyl sulfoxide and acetonitrile solution (1:10), to which 3,4-diaminobenzoic acid and 2,4-dihydroxy benzaldehyde were slowly added. The resulting mixture was kept at 76 °C for 24 hours and the product was isolated by filtration. Yield: 49% (**1-Pt**).

Synthesis 2-hydroxy-4-[2-(piperidinyl) ethoxy] benzaldehyde (L2')

A solution of 2,4-dihydroxybenzaldehyde (500 mg, 3,62 mmol), 1-(2-chloroethyl) piperidine hydrochloride (1330 mg, 7,25 mmol) and potassium carbonate (1252 mg, 9.06 mmol) in acetone was stirred under reflux for 8 hours and a precipitate was formed. The solid was filtered off and washed with acetone. The filtrate was concentrated under pressure to obtain a brown oil which was dried under vacuum. The product was purified with a silica column using a mixture of ethyl acetate: acetone (7:3) as an eluent yielding a light-yellow solid. Yield: 362 mg (40%). **^{1}H-NMR** (400 MHz, DMSO-d_6) δ 11.00 (s br, 1H, OH), 10.00 (s, 1H, CHO), 7.61 (d, 1H, ArH), 6.57 (dd, 1H, ArH), 6.48 (d, 1H, ArH), 4.12 (t, 2H, CH_2O), 2.65 (t, 2H, CH_2N), 2.45-2.35 (m, 4H, piperidine), 1.53-1.44 (m, 4H, piperidine), 1.43-1.33 (m, 2H, piperidine). **^{13}C NMR** (100 MHz, DMSO-d_6): δ 191.13, 165.21, 163.08, 132.26, 116.15, 107.75, 101.32, 66.06, 57.03, 54.33, 25.52, 23.88. **MS-ESI$^+$**: *m/z* 250.14 $[M+H]^+$ (calc: 250.15). **IR**: υ 3065.37 (O–H), 1675.83 (C=O), 1593.90 (C=N). **Anal. Found**. (calcd for $C_{14}H_{19}NO_3$): C 67.25 (67.45), H 7.66 (7.68), N 5.65 (5.62).

Synthesis of 2-Zn

To a solution of 2-hydroxy-4-[2-(ethylpiperidine)ethoxy] benzaldehyde (40 mg, 0,16 mmol) in ethanol, 13 mg (0.08 mmol) of 3,4-diaminobenzoic acid and 10 mg (0.08 mmol) of $Zn(O_2CCH_3)_2 \cdot 2\ H_2O$ were added. The mixture was stirred at room temperature for 24 hours and a precipitate was formed. The yellow solid was filtered, washed with cold ethanol, CH_2Cl_2 and diethyl ether and dried under vacuum. Yield: 49 mg (92%). **^{1}H-NMR** (400 MHz, DMSO-d_6): δ 8.92 (s, 2H, HC=N), 8.27 (s, 1H, Ar–H), 7.84 (s, 2H, Ar–H), 7.39 (d, 1H, Ar–H), 7.30 (d, 1H, Ar–H), 6.18-6.15 (m, 4H, Ar–H), 4.09 (s br, 4H, CH_2O), 2.71 (s br, 4H, CH_2N), 2.61 (s br, 8H, piperidine), 1.56 (s br, 8H, piperidine), 1.42 (s br, 4H, piperidine). **MS-ESI$^+$**: *m/z* 677.23 $[M+H]^+$ (calc: 677.23). **IR**: υ 3700–2400 (O–H), 1612.11 (C=O), 1581.77 (C=N). **Anal. Found**. (calcd for $C_{35}H_{40}N_4O_6Zn{\cdot}2H_2O$): C 58.96 (58.87), H 6.22 (6.21), N 7.83 (7.85).

Method C

Synthesis of 2-Zn

In a Schlenk flask under N_2 atmosphere, **1-Zn** (100 mg, 0.22 mmol), 1-(2-chloroethyl) piperidine hydrochloride (82 mg, 0.44 mmol) and caesium carbonate (180 mg, 0.55 mmol) were added, and the mixture was stirred in solid state during 5 min. Dry DMF (18 mL) was slowly added to the reaction. The solution was stirred at 30 °C for 72 hours. After cooling, the mixture was filtered to remove the excess salts and the solvent was removed under vacuum. The resulting dark red solid was recrystallized twice with a CH_2Cl_2: n-pentane (1:5) mixture to give a yellow solid. Yield: 100 mg (26%).

Synthesis of 2-Ni

Compound **2-Ni** was obtained as a dark red solid using the same procedure from 135 mg (0.3 mmol) of **1-Ni**, 276 mg (1.5 mmol) of 1-(2-chloroethyl) piperidine hydrochloride and 332 mg (2.4 mmol) of caesium carbonate. Yield: 60 mg (30%). **^{1}H-NMR** (400 MHz, DMSO-d_6): δ 8.42 (s, 1H, Ar–H), 8.15 (s, 1H, HC=N), 8.07 (s, 1H, HC=N), 7.16-7.21 (m, 2H, Ar–H), 6.58 (m, 2H, Ar–H), 6.34 (m, 2H, Ar–H), 4.46 (m, 2H, Ar–H), 4.11 (s br, 4H, CH_2O), 2.77 (s br, 4H, CH_2N), 2.49 (s br, 8H, piperidine), 1.61 (s br, 8H, piperidine), 1.46 (s br, 4H, piperidine). **MS-ESI$^+$**: *m/z* 671.24 $[M+H]^+$ (calc: 671.24). **IR**: υ 3700–2400 (O–H), 1615.14 (C=O), 1572.66 (C=N). **Anal. Found**. (calcd for $C_{35}H_{40}N_4O_6Ni{\cdot}H_2O$): C 61.03 (60.98), H 6.13 (6.14), N 8.16 (8.13).

Synthesis of 2-Cu

Compound **2-Cu** was obtained as a green solid using the same procedure from 234 mg (0.5 mmol) of **1-Cu**, 460 mg (2.5 mmol) of 1-(2-chloroethyl) piperidine hydrochloride and 552 mg (4.0 mmol) of caesium carbonate. Yield: 50 mg (30%). **MS-ESI$^+$**: *m/z* 676.24 $[M+H]^+$ (calc: 676.23). **IR**: υ 3700–2400 (O–H), 1606.04 (C=O), 1573.31 (C=N). **Anal. Found**. (calcd for $C_{35}H_{40}N_4O_6Cu{\cdot}2H_2O$): C 58.93 (59.02), H 6.23 (6.21), N 7.89 (7.87).

Research Article
doi.org/10.1002/ejic.202300144

Synthesis of 2-Pt

A suspension of **1-Pt** (70 mg, 0.120 mmol), 1-(2-chloroethyl)piperidine hydrochloride (110 mg, 0.597 mmol), and K_2CO_3 (132 mg, 0.955 mmol) in dry DMF was stirred at 90 °C for 24 h. After cooling, the excess salts were removed by filtration and the solvent was removed under pressure. The resulting dark-red solid was recrystallized with CH_2Cl_2:n-pentane (1:5) to give an orange solid. Yield: 24 mg (25%). **^{1}H-NMR** (400 MHz, DMSO-d_6): δ 9.42 (s, 1H, HC=N), 9.37 (s, 1H, HC=N), 8.88 (s, 1H, Ar–H), 7.88 (m, 2H, Ar–H), 7.73 (d, 1H, Ar–H), 6.59 (m, 2H, Ar–H), 6.48 (m, 2H, Ar–H), 4.10 (s br, 4H, CH2O), 3.22 (s br, 4H, CH2 N), 2.61 (s br, 8H, piperidine), 2.40 (s br, 4H, piperidine) 1.56 (s br, 8H, piperidine), 1.42 (b, 4H, piperidine). **MS-ESI$^+$**: *m/z* 807.26 $[M-H]^+$ (calc: 807.81). **IR**: υ 3700–2400 (O–H), 1612.11 (C=O), 1575.70 (C=N). **Anal. Found**. (calcd for $C_{35}H_{40}N_4O_6Pt{\cdot}2.5H_2O$): C 49.49 (49.29), H 5.32 (5.32), N 6.55 (6.57).

Preparation of Complexes 3-M

Method A

Synthesis of (E)-3-amino-4-((2,4-dihydroxybenzylidene)amino) benzoic acid (L3')[34]

To a solution of 2,4-dihydroxybenzaldehyde (276 mg, 1.01 mmol) in 10 mL of MeOH., 304 mg (1.01 mmol) of 3,4-diamino benzoic acid were added. The mixture was heated in a microwave reactor at 63 °C for 30 minutes and a precipitate was formed. The yellow solid was filtered and dried under vacuum and recrystallized with THF. Yield: 453 mg (68%). mp 195–196 °C. **^{1}H-NMR** (400 MHz, DMSO-d_6): δ 12.78 (s, 1H, Ar–OH), 12.21 (s br, 1H, COOH), 10.21. (s br, 1H, Ar–OH), 8.74 (s, 1H, HC=N), 7.58-7.52 (m, 3H, Ar–H), 6,75 (d, 1H, ArH), 6.40 (dd, 1H, ArH), 6.31 (s, 1H, ArH), 5.76 (s, 2H, NH_2). **^{13}C NMR** (100 MHz, DMSO-d_6): δ 167.41, 162.23, 162.16, 161.48, 146.84, 134.06, 134.00, 128.84, 119.66, 117.95, 113.71, 112.70, 107.79, 102.22. **MS-ESI$^+$**: *m/z* 273.09 $[M+H]^+$ (calc: 273.09). **IR**: υ 3700–2400 (O–H), 1645.49 (C=O), 1618.18 (C=N). **Anal. Found**. (calcd for $C_{14}H_{12}N_2O_4$): C 61.52 (61.76), H 4.46 (4.44), N 10.33 (10.29).

Synthesis of 3-(((E)-2,4-dihydroxybenzylidene)amino)-4-(((E)-2-hydrox-xy-4-(2-(piperidin-1-yl)ethoxy)benzylidene)amino)benzoic acid (L3)

In a 10 mL flask, 63 mg (0,25 mmol) of **L2'** were dissolved in 5 mL of MeOH. Slowly, 68 mg (0,25 mmol) of **L3'** were added to the solution. The mixture was stirred at room temperature for 24 hours and a precipitate was formed. The yellow solid was filtered, washed with methanol and acetone and dried under vacuum. Yield: 83 mg (66%). **^{1}H-NMR** (400 MHz, DMSO-d_6): δ 13.29 (s, 1H, Ar–OH), 13.16 (s, 1H, Ar–OH), 10,32 (s br, 1H, Ar–H), 8.86 (s, 2H, HC=N), 7,89 (m, 2H, Ar–H), 7.59-7.47 (m, 3H, ArH), 6.55 (d, 1H, ArH), 6.50 (s, 1H, ArH), 6.39 (d, 1H, ArH), 6.28 (s, 1H, ArH), 4.13 (s, 2H, CH_2O), 2.69 (s, 2H, CH_2N), 2.50 (s br, 4H, piperidine), 1.50 (s br, 4H, piperidine), 1.38 (s br, 2H, piperidine). **MS-ESI$^+$**: *m/z* 504.21 $[M+H]^+$ (calc: 504.22). **IR**: υ 3700–2400 (O–H), 1621.21 (C=O), 1596.94 (C=N). **Anal. Found**. (calcd for $C_{28}H_{29}N_3O_6{\cdot}$MeOH): C 63.51 (63.48), H 6.59 (6.57), N 7.42 (7.40).

Synthesis of 3-Zn

To a solution of **L3** (125 mg, 0.25 mmol) in 5 mL of methanol, a solution of $Zn(O_2CCH_3)_2{\cdot}2\ H_2O$ (30 mg, 0.25 mmol) in 5 mL of methanol was added. The mixture was stirred under reflux for 1 h and a second equivalent of $Zn(O_2CCH_3)_2{\cdot}2\ H_2O$ was added. This procedure was repeated 3 times and a precipitate was formed. The yellow solid was filtered, washed with cold methanol and dried under vacuum. Yield: 84 mg (59%). **^{1}H-NMR** (400 MHz, DMSO-d_6) δ 9.78 (s, 1H, Ar–OH), 8.92 (s, 1H, N=CH), 8.86 (s, 1H, N=CH), 8.27 (s br, 1H, Ar–H), 7.31 (s br, 2H, Ar–H), 6.20 (m, 2H, Ar–H), 6.05 (s, 2H, ArH), 4.08 (s br, 2H, CH_2O), 2.68 (s br, 2H, CH_2N), 2.60 (s br, 4H, piperidine), 1.51 (s br, 4H, piperidine), 1.39 (s br, 2H, piperidine). **MS-ESI$^+$**: *m/z* 566.12 $[M+H]^+$ (calc: 566.13). **IR**: υ 3700–2400 (O–H), 1615.14 (C=O), 1584.80 (C=N). **Anal. Found**. (calcd for $C_{28}H_{27}N_3O_6Zn{\cdot}H_2O$): C 57.81 (57.50), H 4.98 (5.00), N 7.20 (7.18).

Method B

Synthesis of 3-Ni

L2' (21 mg, 0.076 mmol), **L3'** (19 mg, 0.076 mmol) and $Ni(O_2CCH_3)_2{\cdot}4\ H_2O$ (19 mg, 0.076 mmol) were dissolved in 5 mL of methanol. An additional equivalent of $Ni(O_2CCH_3)_2{\cdot}4\ H_2O$ was added each hour for 4 h. The mixture was stirred at room temperature for 24 hours and a precipitate was formed. The red solid was filtered, washed with methanol and dried under vacuum. Yield: 26 mg (59%). **^{1}H-NMR** (400 MHz, DMSO-d_6): δ 10.28 (s, 1H, Ar–OH), 8.70 (s br, 2H, N=CH), 8.52 (s br, 1H, Ar–H), 8.10 (s br, 1H, Ar–H), 7.77 (s br, 1H, Ar–H), 7.54 (d, 1H, Ar–H), 7.47 (d, 1H, Ar–H), 6.40 (s, 1H, Ar–H), 6.33 (d, 1H, ArH), 6.20 (m, 2H, Ar–H), 4.10 (s br, 2H, CH2O), 2.68 (s br, 2H, CH2 N), 2.67 (s br, 4H, piperidine), 1.51 (s br, 4H, piperidine), 1.38 (s br, 2H, piperidine). **MS-ESI$^+$**: *m/z* 560.13 $[M+H]^+$ (calc: 560.14). **IR**: υ 3700–2400 (O–H), 1609.07 (C=O), 1581.77 (C=N). **Anal. Found**. (calcd for $C_{28}H_{27}N_3O_6Ni{\cdot}$MeOH): C 58.72 (58.81), H 5.26 (5.28), N 7.12 (7.09).

Synthesis of 3-Cu

Compound 3-Cu was obtained as a green solid using the same procedure from **L2' (**21 mg, 0.076 mmol), **L3'** (19 mg, 0.076 mmol) and $Cu(O_2CCH_3)_2{\cdot}H_2O$ (14 mg, 0.076 mmol). Yield: 30 mg (70%). **MS-ESI$^+$**: *m/z* 565.13 $[M+H]^+$ (calc: 565.13). **IR**: υ 3700–2400 (O–H), 1590.87 (C=O), 1533.22 (C=N). **Anal. Found**. (calcd for $C_{28}H_{27}N_3O_6Cu\cdot 2.5H_2O$): C 55.29 (55.12), H 5.30 (5.29), N 6.92 (6.89).

Oligonucleotides

The labelled *c-myc* oligonucleotide (FAM-GAG-GGT-GGG-GAG-GGT-GGG-GAA–G-TAMRA) was purchased from Eurogentec (Belgium) as lyophilised solids (RP-Cartridge Gold purification) and dissolved in MilliQ water at a concentration of 200 μM, as determined by UV-vis spectroscopy at 260 nm (using the extinction coefficient $\varepsilon = 232\,000$ in $L\,mol^{-1}\,cm^{-1}$ given by the manufacturer) and diluted to 20 μM in the appropriate buffer. For st-DNA and ct-DNA the concentration was determined by base pair ($\varepsilon = 13\,200\ L\,mol^{-1}\,cm^{-1}$).

FRET melting assay

The doubly labelled DNA strand tested in the fluorescence resonance energy transfer (FRET) assay (FAM/TAMRA labelling) were prepared as 20 μM stock solutions in MilliQ water and a 0.4 μM DNA working solution was obtained by heating the oligonucleotide at 95 °C for 5 min in annealing buffer (1 mM KCl, 99 mM LiCl, 10 mM LiCacodylate, pH 7.4), followed by slow cooling over 4 h. All compounds were stored as DMSO stock solutions (2 mM) at −20 °C. Prior to the experiment, solutions were thawed and diluted in cacodylate buffer on the day of use.

FRET melting experiments were carried out on an Agilent Stratagene Mx3005P qPCR machine equipped with a 96 well plate, a quartz tungsten halogen lamp as the excitation source, a single photomultiplier tube for detection and a Peltier-based thermal cycler. The protocol described by Mergny et al. was followed.[35] Samples were prepared in 96 well plate (Agilent Technologies, UK) and the measurements were carried out in triplicates. For the FAM-TAMRA system an excitation range of 492–516 nm and an emission range of 556–580 nm was used. A temperature gradient of 0.5 °C/30 sec was applied, and fluorescence readings were taken at 0.5 °C intervals from 25 °C to 95 °C. Data analysis was performed with the program OriginPro 9.1. The melting temperature was calculated by fitting the normalized fluorescence data with a sigmoidal function using a dose-response model and checking the temperature value for $y = 0.5$. ΔT_m was reported as the difference between the DNA melting temperature in the absence of any compound and the DNA melting with different concentrations of the compound.

To each well in a 96 well plate (Agilent Technologies, UK), 20 μL of 0.4 μM FAM-TAMRA labelled DNA and 20 μL of the 1 μM ligand solution were added. As a control, the FRET melting assays were also carried out in the absence of the complex solutions.

Ligand solutions (10 μM) in buffer were prepared from DMSO stock solutions, followed by further dilution to 0.4, 0.8, 2.0, 4.0, 8.0 μM. For the sample preparation (final volume of 40 μL) 20 μL 0.4 μM DNA were added to each well in a 96 well plate, followed by 20 μL ligand dilution with increasing concentrations. As a control, one sample with ligand-free buffered solution was used. After thorough mixing, samples were measured as described above.

FRET competition assay

CT-DNA stocks were diluted to 24 μM and 480 μM, ligand stocks to 4 μM in the appropriate buffer. Six solutions containing no ligand, ligand but no CT-DNA and increasing concentrations of CT-DNA (0.6 to 120 μM) were prepared. After gentle mixing 20 μL of those solutions were added to 20 μL of labelled DNA into the 96 well plate. Final concentration of labelled DNA was 0.2 μM and ligand 2.0 μM. Measurements were performed in the same way as the FRET melting.

Emission titrations to determine DNA binding affinity

DNA stock solutions were prepared using Tris phosphate buffer (10 mM, pH 7.4) and concentrations were determined using an Agilent Cary UV 60 spectrometer. Prior to use, KCl (100 mM) was added to each G4 DNA stock (purchased from IDT or Eurogentec – see ESI for exact sequences and commerical source) before annealing at 95 °C for 5 minutes and cooling to room temperature overnight. CT-DNA was obtained from Sigma-Aldrich and prepared using Tris phosphate buffer (10 mM, 100 mM KCl, pH 7.4).

Emission titrations were performed with 2 μM of **2-Pt** in a Tris phosphate buffer (10 mM, 100 mM KCl, pH 7.4) with concentrations of quadruplex DNA ranging from 0 to 12 μM (concentration of strands), and CT-DNA from 0 to 24 μM (concentration of base pairs). This was performed using a 96 well plate with volumes of 100 μL, using a Clariostar plus plate reader following excitation at 380 nm. The changes in emission were plotted against the oligonucleotide concentration for each complex and fitted using GraphPad Prism 9 One site specific binding: $Y = B_{max}*X/(K_d + X)$. Kd was then converted to K_a ($K_a = 1/K_d$) and error was measured by the relative standard error.

Computer docking studies

Complex geometries were optimised to find the lowest energy conformation using DFT B3LYP with basis sets LANL2DZ for platinum atoms, and 6–31G for all other atoms and compared with crystallographic literature values.[36] The same DFT methods were used for energy and molecular orbital calculations. The optimised structures were then used for docking simulations. These were performed in AutoDock4 using default settings. PDB structures of DNA were obtained from the protein databank (see ESI for exact sequences). Some G4 structures used in docking contained a bound ligand which was removed prior to docking. These include c-myc (2L7V), HTelo (5MVB), kras (7X8M), and HTG4 (2MB3). The sequences of these structures were otherwise unchanged. Structures including a bound ligand were not available for BCL-2 (6ZX7), ckit1 (4WO2), and ckit2 (2KYP). Results were visualised using AutoDockTools.

Acknowledgements

The authors are grateful to Project PID2019-104121GB–I00 funded by Ministerio de Ciencia e Innovación of Spain MCIN/AEI/10.13039/501100011033. This article is based on work from COST Actions CA 17140 "Cancer Nanomedicine from the Bench to the Bedside" and CA18202-NECTAR supported by COST (European Cooperation in Science and Technology). ADC acknowledges the financial support from "La Sapienza" (grant no. RM11916B891 A9986). J.B.R. acknowledges the financial support from CONACYT and M.B. the UK's Engineering and Physical Sciences Research Council (EPSRC grants EP/S023232/1).

Conflict of Interests

The authors declare no conflict of interest.

Data Availability Statement

The data that support the findings of this study are available in the supplementary material of this article.

Keywords: Asymmetric ligands · bioinorganic chemistry · metal salophen complexes · quadruplex DNA · supramolecular chemistry

[1] a) P. A. Vigato, S. Tamburini, *Coord. Chem. Rev.* **2004**, *248*, 1717–2128; b) W. Qin, S. Long, M. Panunzio, S. Biondi, *Molecules* **2013**, *18*, 12264–12289.
[2] P. G. Cozzi, *Chem. Soc. Rev.* **2004**, *33*, 410–421.
[3] a) S. Di Bella, *Dalton Trans.* **2021**, *50*, 6050–6063; b) S. J. Wezenberg, A. W. Kleij, *Angew. Chem. Int. Ed.* **2008**, *47*, 2354–2364.
[4] S. Kumar, D. N. Dhar, P. N. Saxena, *J. Sci. Ind. Res.* **2009**, *68*, 181–187.
[5] M. N. Uddin, S. S. Ahmed, S. M. R. Alam, *J. Coord. Chem.* **2020**, *73*, 3109–3149.
[6] A. Arunadevi, N. Raman, *J. Coord. Chem.* **2020**, *73*, 2095–2116.
[7] J. G. Muller, S. J. Paikoff, S. E. Rokita, C. J. Burrows, *J. Inorg. Biochem.* **1994**, *54*,199–206.
[8] C. J. Burrows, S. E. Rokita, *Acc. Chem. Res.* **1994**, *27*, 295–301.

[9] J. E. Reed, A. A. Arnal, S. Neidle, R. Vilar, *J. Am. Chem. Soc.* **2006**, *128*, 5992–5993.
[10] A. Arola-Arnal, J. Benet-Buchholz, S. Neidle, R. Vilar, *Inorg. Chem.* **2008**, *47*, 11910–11919.
[11] N. H. Campbell, N. H. Abd Karim, G. N. Parkinson, M. Gunaratnam, V. Petrucci, A. K. Todd, R. Vilar, S. Neidle, *J. Med. Chem.* **2012**, *55*, 209–222.
[12] A. Ali, M. Kamra, S. Roy, K. Muniyappa, S. Bhattacharya, *Bioconjugate Chem.* **2017**, *28*, 341–352.
[13] A. Terenzi, D. Lötsch, S. van Schoonhoven, A. Roller, C. R. Kowol, W. Berger, B. K. Kepplera, G. Barone, *Dalton Trans.* **2016**, *45*, 7758–7767.
[14] L. Lecarme, E. Prado, A. De Rache, M.-L. Nicolau-Travers, G. Gellon, J. Dejeu, T. Lavergne, H. Jamet, D. Gomez, J.-L. Mergny, E. Defrancq, O. Jarjayes, F. Thomas, *ChemMedChem* **2016**, *11*,1133–1136.
[15] K. J. Davis, C. Richardson, J. L. Beck, B. M. Knowles, A. Guédin, J.-L. Mergny, A. C. Willis, S. F. Ralph, *Dalton Trans.* **2015**, *44*, 3136–3150.
[16] D. Rhodes, H. J. Lipps, *Nucleic Acids Res.* **2015**, *43*, 8627–8637.
[17] R. Hansel-Hertsch, M. Di Antonio, S. Balasubramanian, *Nat. Rev. Mol. Cell Biol.* **2017**, *18*, 279–284.
[18] J. Robinson, F. Raguseo, S. P. Nuccio, D. Liano, M. Di Antonio, *Nucleic Acids Res.* **2021**, *49*, 8419–8431.
[19] S. Neidle, *J. Med. Chem.* **2016**, *59*, 5987–6011.
[20] S. Neidle, *Nat. Chem. Rev.* **2017**, *1*, 10.
[21] L. Leoni, A. Dalla Cort, *Inorganics* **2018**, *6*, 42.
[22] M. Cano, L. Rodríguez, J. C. Lima, F. Pina, A. Dalla Cort, C. Pasquini and L. Schiaffino, *Inorg. Chem.* **2009**, *48*, 6229–6235.
[23] A. Dalla Cort, P. De Bernardin, G. Forte, F. Yafteh Mihan, *Chem. Soc. Rev.* **2010**, *39*, 3863–3874.
[24] S. Bartocci, F. Sabaté, F. Yafteh Mihan, R. Bosque, L. Rodríguez, A. Dalla Cort, *Supramol. Chem.* **2017**, *29*, 922–927.
[25] F. Sabaté, R. Gavara, I. Giannicchi, R. Bosque, A. Dalla Cort, L. Rodríguez, *New J. Chem.* **2016**, *40*, 5714–5721.
[26] F. Sabaté, I. Giannicchi, L. Acón, A. Dalla Cort, L. Rodríguez, *Inorg. Chim. Acta* **2015**, *434*, 1–6.
[27] D. Xie, J. Jing, Y.-B. Cai, J. Tang, J.-J. Chen, J.-L. Zhang, *Chem. Sci.* **2014**, *5*, 2318–2327.
[28] G. Consiglio, S. Failla, I. P. Oliveri, R. Purrello, S. Di Bella, *Dalton Trans.* **2009**, 10426–10428.
[29] G. Consiglio, I. P. Oliveri, S. Cacciola, G. Maccarrone, S. Failla, S. Di Bella, *Dalton Trans.* **2020**, *49*, 5121–5133.
[30] I. Giannicchi, R. Brissos, D. Ramos, J. de Lapuente, J. C. Lima, A. Dalla Cort, L. Rodríguez, *Inorg. Chem.* **2013**, *52*, 9245–9253.
[31] R. Brissos, D. Ramos, J. C. Lima, F. Yafteh Mihan, M. Borrás, J. de Lapuente, A. Dalla Cort, L. Rodríguez, *New J. Chem.* **2013**, *37*, 1046–1055.
[32] G. Consiglio, I. P. Oliveri, S. Failla, S. Di Bella, *Molecules* **2019**, *24*, 2514.
[33] J. Zhang, L. Wang, A. Zhong, G. Huang, F. Wu, D. Li, M. Teng, J. Wang, D. Han, *Dyes Pigm.* **2019**, *162*, 590–598.
[34] N. C. Ramos, A. Echevarria, A. Valbon, A. J. Bortoluzzi, G. P. Guedes, C. E. Rodrigues-Santos, *Cogent Chem.* **2016**, *2*, 1207863.
[35] J.-L. Mergny, L. Lacroix, *Curr. Protoc. Nucleic Acid Chem.* **2009**, *37*, 1–15.
[36] M. T. Proetto, W. Liu, A. Molchanov, W. S. Sheldrick, A. Hagenbach, U. Abram, R. Gust, *ChemMedChem* **2014**, *9*, 1176–1187.

Manuscript received: March 17, 2023
Revised manuscript received: July 19, 2023
Accepted manuscript online: July 20, 2023
Version of record online: August 1, 2023